Native Approach to Controlled-Z Gates in Inductively Coupled Fluxonium Qubits

Xizheng Ma,[1,*] Gengyan Zhang,[1,*] Feng Wu,[1,*] Feng Bao,[1] Xu Chang,[1] Jianjun Chen,[1,†] Hao Deng,[1] Ran Gao,[1] Xun Gao,[2] Lijuan Hu,[1] Honghong Ji,[1] Hsiang-Sheng Ku,[1,‡] Kannan Lu,[1] Lu Ma,[1] Liyong Mao,[1] Zhijun Song,[1] Hantao Sun,[1] Chengchun Tang,[1] Fei Wang,[1] Hongcheng Wang,[1] Tenghui Wang,[1] Tian Xia,[1] Make Ying,[1] Huijuan Zhan,[1] Tao Zhou,[1] Mengyu Zhu,[1] Qingbin Zhu,[1] Yaoyun Shi,[2] Hui-Hai Zhao,[3,§] and Chunqing Deng[1,‖]

[1]*DAMO Quantum Laboratory, Alibaba Group, Hangzhou, Zhejiang 311121, China*
[2]*DAMO Quantum Laboratory, Alibaba Group USA, Bellevue, Washington 98004, USA*
[3]*DAMO Quantum Laboratory, Alibaba Group, Beijing 100102, China*

The fluxonium qubits have emerged as a promising platform for gate-based quantum information processing. However, their extraordinary protection against charge fluctuations comes at a cost: when coupled capacitively, the qubit-qubit interactions are restricted to XX interactions. Consequently, effective ZZ or XZ interactions are only constructed either by temporarily populating higher-energy states, or by exploiting perturbative effects under microwave driving. Instead, we propose and demonstrate an inductive coupling scheme, which offers a wide selection of native qubit-qubit interactions for fluxonium. In particular, we leverage a built-in, flux-controlled ZZ interaction to perform qubit entanglement. To combat the increased flux-noise-induced dephasing away from the flux-insensitive position, we use a continuous version of the dynamical decoupling scheme to perform noise filtering. Combining these, we demonstrate a 20 ns controlled-z gate with a mean fidelity of 99.53%. More than confirming the efficacy of our gate scheme, this high-fidelity result also reveals a promising but rarely explored parameter space uniquely suitable for gate operations between fluxonium qubits.

Repeated demonstrations of long coherence times [1–3] and high-fidelity gate operations [4–8] over the years have firmly established the fluxonium qubits as a promising platform for gate-based quantum computation. Compared to transmons, fluxonium qubits have two obvious advantages: their low transition energies between the ground and first excited state allows for better coherence times by reducing the effect of dielectric loss [2,9,10]; and their large anharmonicity offers a broad spectral range for qubit operations without leakage to higher (noncomputational) excited states [4,5]. Most experiments, therefore, have treated fluxonium as an improved version of transmon by opting for a capacitive coupling scheme standard for charge-type qubits [11]. However, the fluxonium's complete lack of energy dispersion in charge basis, while providing an excellent protection against charge-noise-induced dephasing, means that any interaction mediated through charge is restricted to the transverse direction of the qubit. Although such XX interaction can be used to perform iSWAP-like gates [4,6], it precludes easy access to a broader range of two-qubit operations such as controlled-z (cz) or controlled-NOT CNOT gates. Instead, an effective ZZ interaction needs to be constructed [6,7,12–14] by temporarily populating the transmonlike higher excited states, whose short coherence times ultimately limit the fidelity of the gates. Alternatively, a second-order effect of the driven dynamics can be exploited [5,15] to create an

effective XZ coupling, but such schemes have to balance slow gate speed with large unwanted interactions.

At its core, fluxonium qubits belong to the family of flux qubits, and are therefore most naturally coupled inductively [Fig. 1(a)]. All flux qubits are essentially superconducting loops interrupted by Josephson junctions. When an external flux Φ close to half-flux quantum $\Phi_0/2$ is applied to the loop, persistent currents $\pm I_p$ circulate the loop in opposite directions, expelling or pulling additional external flux to maintain flux quantization. These persistent current states are coupled via the Josephson junction at a tunneling energy Δ [Fig. 1(b)]. By controlling the magnetic energy difference between these states $\epsilon = 2I_p(\Phi - \Phi_0/2)$, Φ determines the qubit energy $\hbar\omega_q = \sqrt{\epsilon^2 + \Delta^2}$. More importantly, it also determines the orientation [16,17] of the current operator $\hat{I}$ [18] flowing across the junction with respect to the energy quantization axis $\hat{\sigma}_z$ of the qubit [Fig. 1(c)]:

$$\hat{I} = I_p(\cos\theta\hat{\sigma}_z - \sin\theta\hat{\sigma}_x), \quad (1)$$

where $\theta = \arctan(\Delta/\epsilon)$ is the mixing angle between the tunneling energy and the magnetic energy. At $\Phi = \Phi_0/2$, the qubit energy is first order insensitive to Φ, and $\hat{I}$ is perpendicular to the energy quantization axis $\hat{\sigma}_z$. Away from the degeneracy position, fluctuations in the current not
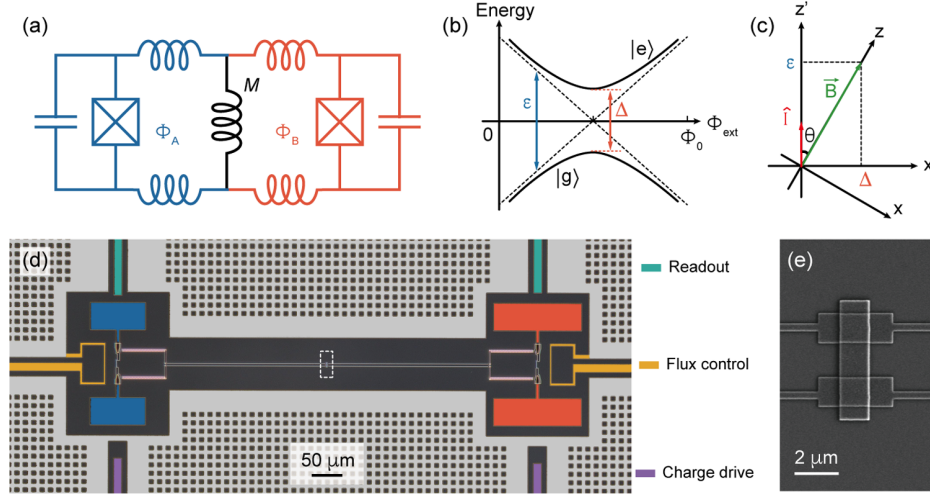
FIG. 1. Inductively coupled fluxonium pair. (a) A pair of fluxonium qubits are coupled inductively though a mutual inductance M, creating an interaction of the form $M\hat{I}_A\hat{I}_B$, where $i = A$ or B indexes the qubit and $\hat{I}_i$ is the qubit's current operator. Each qubit can be individually controlled with an external flux Φ_i applied to its superconducting loop with total inductance L_i. (b) For each qubit, its ground ($|g\rangle$) and excited ($|e\rangle$) states are superpositions of two persistent current states (dashed lines) with equal currents circulating the loop in opposite directions. Defining the average magnetic energy of the two persistent current states to be zero, their energy difference ϵ is linearly dependent on Φ applied to the qubit. The degeneracy between these states at $\Phi = \Phi_0/2$ is lifted by the Josephson junction with a tunneling energy Δ. (c) Such a system resembles [16] a spin of unit dipole moment subjected to a fictitious magnetic field $\vec{B} = \Delta\hat{x}' + \epsilon\hat{z}'$, where $\hat{z}'$ aligns with $\hat{I}$ (red). By adjusting ϵ via Φ, we can access a diverse range of interactions by controlling the orientation of the qubit energy quantization axis $\hat{\sigma}_z$, aligned along the net magnetic field $\hat{z}$ (green) and rotated by an angle θ with respect to the current operator $\hat{I}$. (d) False colored optical image of the inductively coupled fluxonium pair. The white dashed rectangle locates the mutual inductance, created by a galvanic connection that shares two junctions between the two fluxonium loops. (e) Scanning electron micrograph showing the two shared overlap [37] junctions.

only drives qubit excitation but also alters the qubit energy. Naturally, when a pair of flux qubits are connected via a mutual inductance M, circulating currents in one qubit induces current in the other qubit, creating a coupling of the form $M\hat{I}_i\hat{I}_j$, where the subscripts index the qubits.

Indeed, inductive coupling offers a diverse range of entangling interactions via the control of the external flux Φ applied to the qubits. These interactions are partly investigated by the early proposals [17,38–43] concerned with connecting the prototypical flux qubits [38]. However, impeded by their extreme sensitivity to flux noise, these flux qubits saw limited application in gate-based quantum computing and have largely pivoted to the field of quantum annealing [44–47]. The few demonstrations [8,48,49] of gate-based operations are limited to the flux-degeneracy position, where the lack of first-order flux dispersion alleviates the qubit decoherence but again restricts the qubit interactions to the transverse directions. By reducing the persistent currents I_p with the increased loop inductance, fluxonium qubits significantly reduce their sensitivity to flux noise [50,51], paving the way toward high-fidelity entangling operations that require temporary excursions away from the flux-degeneracy position.

In this Letter, we inductively couple a pair of fluxonium qubits and demonstrate high-fidelity gate operations by leveraging a native ZZ interaction that is only switched on when both qubits are biased away from their flux-degeneracy positions. As shown in Figs. 1(d) and 1(e), the inductive coupling is created by a galvanic connection that shares part of the junction arrays forming the loop inductors. Under external fluxes Φ_A and Φ_B close to $\Phi_0/2$ [18], we can write down the general form of the system's Hamiltonian,

$$H(\Phi_A, \Phi_B) = \frac{\hbar}{2}\sum_{i=A,B}\omega_i\hat{\sigma}_z^i + J\sin\theta_A\sin\theta_B\hat{\sigma}_x^A\hat{\sigma}_x^B$$
$$- J\sum_{i\neq j}\cos\theta_i\sin\theta_j\hat{\sigma}_z^i\hat{\sigma}_x^j$$
$$+ J\cos\theta_A\cos\theta_B\hat{\sigma}_z^A\hat{\sigma}_z^B, \qquad (2)$$

where $J/\hbar = MI_p^A I_p^B/\hbar \approx 2\pi \times 19$ MHz is the inductive coupling strength, and $\theta_i = \arctan(\Delta_i/\epsilon_i(\Phi_i))$ is the mixing angle of the ith qubit with $\cos\theta_i = 0$ at $\Phi_i = \Phi_0/2$. In this Hamiltonian, the first line contains the always-on transverse interaction. The second line describes an XZ interaction when either qubit is biased away from its flux-degeneracy position. When modulated at an appropriate frequency [52,53], such a native XZ coupling provides a promising path toward a fast controlled-NOT gate. But for near-static flux modulations considered in this Letter, qubit j merely acquires an i-state-dependent rotation of angle

$(2J/\hbar\omega_j)\cos\theta_i\sin\theta_j\hat{\sigma}_z^i$ that has little consequence for $J \ll \hbar\omega_j$ [18]. Finally, when both qubits are biased away from the half-flux position, the ZZ interaction in the last line of Eq. (2) induces qubit frequency shifts $\delta\omega_i = 2g_{zz}\langle\hat{\sigma}_z^j\rangle$ dependent on the state of the other qubit, defining the shorthand $\hbar g_{zz} = J\cos\theta_A\cos\theta_B$.

To confirm this system Hamiltonian, we perform spectroscopic measurements on qubit A at a constant $\Phi_A = 0.458\Phi_0$ [Fig. 2(a)] while varying the external flux Φ_B applied to qubit B. When the two qubits come into resonance, the transverse interaction causes a coherent exchange of qubit energy, which manifests as level repulsions at $\Phi_B = 0.5 \pm 0.062\Phi_0$. Away from the resonant positions, this coherent exchange is suppressed by the qubit detuning. Instead, the effect of the ZZ interaction dominates. Because qubit B is initialized in a thermal state with approximately 24% probability of finding $|e\rangle$, the spectrum of qubit A is double peaked, where the more and less prominent peaks respectively correspond to qubit A's frequency when qubit B is in state $|g\rangle$ and $|e\rangle$. The distance between these peaks therefore directly corresponds to g_{zz}, adjustable via the control of the external flux.

Leveraging this flux-controlled ZZ coupling, we implement two-qubit conditional-phase gates by simultaneously applying flux pulses on $\Phi_{A,B}(t)$ to both qubits. Using a Ramsey-type experiment [Fig. 2(b)], we characterize the accumulation speed of the conditional phase under flux pulses of length τ,

$$v_\phi = \frac{1}{\tau}\int_0^\tau 4g_{zz}(\Phi_A(t),\Phi_B(t))dt. \qquad (3)$$

Figure 2(c) shows v_ϕ as a function of how far the qubits are biased away from the half-flux position under square pulses

of amplitude $\delta\Phi_{A,B}$ and duration $\tau = 200$ ns. In this experiment, we enveloped the square pulses with a tanh function with a characteristic rise time $t_r = 2$ ns, slow enough to ensure that the flux modulations do not significantly alter the qubits' excitation via diabatic passages [18]. Note that when either qubit is kept at the half-flux position ($\delta\Phi_i = 0$), a conditional phase still accumulates slowly. Indeed, this slow accumulation is the result of a residual ZZ coupling g_{zz}^{res}, caused by transverse interactions between the computational states and higher-energy qubit states [12,15]. Importantly, this residual ZZ coupling does not contribute any two-qubit gate errors because it is naturally absorbed into Eq. (3) during gate calibration. Meanwhile, $g_{zz}^{\mathrm{res}} \approx 2\pi \times 17.4$ kHz at the idle position [18], where both qubits are parked at $\Phi_0/2$, contributes a negligible error in the range of 10^{-5} to single-qubit operations. We stress that, because we leverage a native ZZ interaction that is first order to the coupling strength J, we could easily attain a large on-off ratio in g_{zz} close to 10^3 without relying on demanding cancellation engineering [5–7,13,15]. Indeed, by simply increasing the distance of both qubits from $\Phi_0/2$, we can drastically increase the accumulation speed of the conditional phase and perform two-qubit CZ gates ($v_\phi\tau = \pi$) as fast as 9 ns. However, this exceptional gate speed comes at the cost of increased qubit sensitivity to flux noise and reduced coherence times.

To combat the effect of flux noise during two-qubit gate operations, we embed a continuous version of the dynamical decoupling scheme [54] to our flux-control pulses. Specifically, we sinusoidally modulate both flux pulses at frequency ω_m with equal phase, resulting in a near-sinusoidal modulation on the slope of either qubit's flux dispersion $\mathcal{D}_i = \partial\omega_i/\partial\Phi_i$, which averages to zero over integer periods [Fig. 3(a)]. Because its noise-filtering
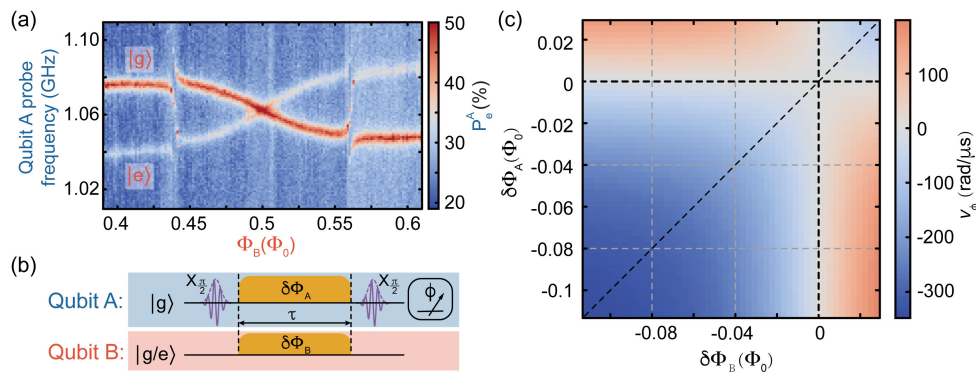

FIG. 2. A native ZZ interaction allows for conditional-phase gates. (a) The spectrum of qubit A is measured as a function of the external flux Φ_B applied to qubit B, while $\Phi_A = 0.458\Phi_0$ is kept as a constant. As a result of the native ZZ interaction, qubit A's resonant frequency is shifted in opposite directions when qubit B is prepared in either $|g\rangle$ or $|e\rangle$. Here, qubit B is prepared in a mixed state with approximately 24% probability in $|e\rangle$, leading to a double-peaked spectrum where the more prominent peak corresponds to qubit B in $|g\rangle$. Additionally, level repulsions can be observed when the two qubits come into resonance at $\Phi_B = 0.5 \pm 0.062\Phi_0$. (b) Using a Ramsey-type experiment, we measure the conditional phase ϕ accumulated on qubit A when we bias both qubits away from $\Phi_0/2$ using the square pulse of amplitude $\delta\Phi_{A,B}$ for duration τ. (c) As a function of the pulse amplitudes, we plot the measured accumulation speed of the conditional phase $v_\phi = \phi/\tau$.
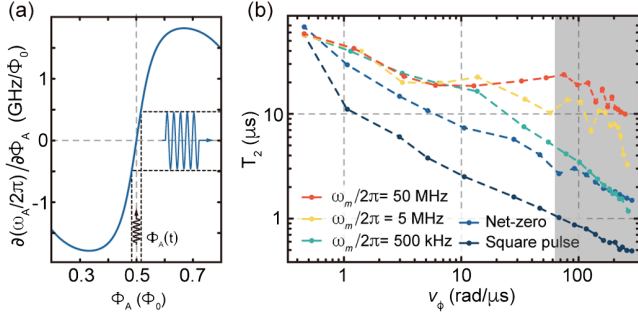
FIG. 3. Using dynamical decoupling to combat flux-noise induced dephasing. (a) The first-order derivative of qubit A's frequency dispersion, $\partial\omega_A/\partial\Phi_A$, is plotted as a function of Φ_A. A sinusoidal flux modulation about $\Phi_0/2$ produces an approximately-sinusoidal modulation of $\partial\omega_A/\partial\Phi_A$, which averages to 0 over integer periods. (b) We measure the characteristic decoherence times (T_2) of qubit A under different flux modulations $\Phi_A(t)$ while qubit B is kept at $\Phi_0/2$. For easy comparison, the amplitude of the flux modulation expressed in v_ϕ had the same flux modulation applied to both qubits $[\Phi_A(t) = \Phi_B(t)]$. The shaded region corresponds to v_ϕ large enough to support CZ gates under 50 ns.
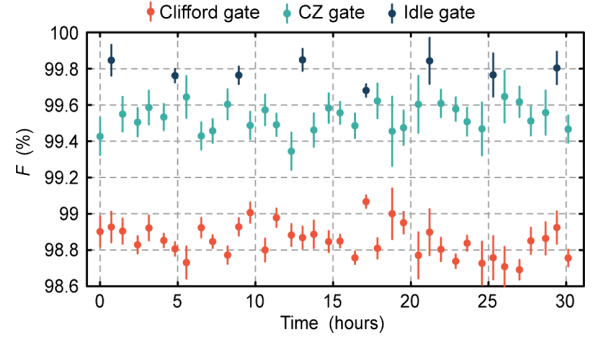

FIG. 4. Gate performance. The gate performances are monitored over a period of 30 h using the standard RB techniques. The error bars correspond to fitting uncertainties.

function is given by the Fourier transformation of the time-dependent $\mathcal{D}(t)$ [55], the qubit dephasing becomes sensitive only to a narrow region of noises with frequencies close to ω_m [18]. Compared to a net-zero decoupling scheme [56,57], where each flux pulse consists of two back-to-back square pulses of equal duration but opposite amplitude, our scheme provides an *in situ* selection of noise frequency while requiring only microwave controls. It is important to note that, because $\hbar\mathcal{D}_i = 2I_p^i \cos\theta_i$, this energy dispersion to external flux is precisely the source of the native ZZ interaction we exploit in two-qubit gates: $g_{zz} \propto \mathcal{D}_A\mathcal{D}_B$. Yet, while our sinusoidal flux modulations average the energy dispersion of either qubit to zero to reduce dephasing, their correlation nevertheless preserves a nonzero ZZ interaction, or v_ϕ, averaged over integer periods. In Fig. 3(b), we demonstrate the efficacy of our dynamical decoupling scheme by measuring qubit A's characteristic decoherence time T_2 under different flux pulses $\Phi_A(t)$ while qubit B is kept at $\Phi_0/2$. For easy comparison [18], the amplitude of $\Phi_A(t)$ is expressed in v_ϕ had both qubits been simultaneously modulated with the same pulse $[\Phi_B(t) = \Phi_A(t)$, diagonal dashed-line in Fig. 2(c)]. Because the qubit dephasing is dominated by $1/f$-flux noise, a clear improvement in T_2 can be observed when the modulation frequency is increased from 500 kHz to 50 MHz. Compared to the case without any dynamical decoupling scheme, the sinusoidal flux modulation improves the coherence time of qubit A by more than an order of magnitude at modulation amplitudes large enough to support fast CZ gates under 50 ns (shaded region).

Employing the sinusoidal dynamical decoupling with $\omega_m = 2\pi \times 50$ MHz, we calibrate a 20 ns CZ gate.

The detailed calibration process can be found in the Supplemental Material [18]. Unfortunately, we suffer from relatively large flux-pulse distortions that require us to append another 20 ns idle time after every CZ gate, effectively doubling our gate time.

Nevertheless, we demonstrate in Fig. 4 our ability to perform high-fidelity gate operations using randomized benchmarking (RB) [58,59]. Monitored over 30 h, we measure a mean Clifford fidelity of $\overline{F_C} = 98.85 \pm 0.08\%$, and a mean CZ gate fidelity of $\overline{F_{CZ}} = 99.53 \pm 0.07\%$, where the uncertainty intervals capture the time fluctuations in the measured fidelities. Because our device suffers from serious TLS poisoning whose effect fluctuates over time [18], it is immensely difficult to accurately predict the decoherence limit of our CZ gate. Instead, we provide a sense of the decoherence effect on the gate fidelity by measuring the mean $\overline{F_{\text{idle}}} = 99.78 \pm 0.05\%$ of a 40 ns idle gate, limited by the coherence times at the idle position [18]. In doing so, we find that approximately half of our CZ gate error comes from decoherence sources that also suppress our qubit coherence times at the degeneracy positions to below 100 µs [18], a subpar performance for fluxonium qubits. Improvements in this performance or reductions in the idle time after each CZ gate therefore could significantly improve our gate fidelities.

More than confirming the efficacy of our gate scheme, our high-fidelity result also reveals a promising but rarely explored parameter space for gate operations. Whereas transmons traded away rich interactions similar to those described in Eq. (2) in favor of an improved coherence time, prototypical flux qubits simply suffer too much decoherence to effectively leverage them. Because of their reduced sensitivity to flux noise compared to the prototypical flux qubits, fluxonium qubits can be operated away from their degeneracy positions, and are therefore uniquely suited to exploit the diverse interactions enabled by inductive-coupling for gate operations.

In summary, we demonstrated a particular synergy between fluxonium qubits and inductive coupling schemes that leads to a native ZZ interaction when both qubits are

biased away from the flux-degeneracy positions. By adjusting the external flux applied to the qubits, we can tune the ZZ-interaction strength over 3 orders of magnitude, enabling fast entangling operations with minimal adverse effects to single-qubit operations. Finally, by embedding a sinusoidal dynamical decoupling scheme into the control sequences, we suppressed the additional dephasing introduced by the two-qubit operations and demonstrated high-fidelity CZ gates that does not involve higher energy states.

Looking forward, tunable couplers based on inductively coupled SQUIDs or fluxonium qubits [8,60] may be a prerequisite for performing the quantum operations demonstrated in this Letter at a much larger scale. Alternatively, the thus far neglected native XZ interactions may also hold a promising path toward highly scalable [15] entangling operations.

---

[*]These authors contributed equally to this work.

[†]Present address: Xinxiao Electronics Inc., Hangzhou, China.

[‡]Present address: IQM Quantum Computers, 80992 Munich, Germany.

[§]zhaohuihai@gmail.com

[‖]dengchunqing@gmail.com

[1] I. M. Pop, K. Geerlings, G. Catelani, R. J. Schoelkopf, L. I. Glazman, and M. H. Devoret, Nature (London) **508,** 369 (2014).

[2] H. Zhang, S. Chakram, T. Roy, N. Earnest, Y. Lu, Z. Huang, D. K. Weiss, J. Koch, and D. I. Schuster, Phys. Rev. X **11,** 011010 (2021).

[3] A. Somoroff, Q. Ficheux, R. A. Mencia, H. Xiong, R. Kuzmin, and V. E. Manucharyan, Phys. Rev. Lett. **130,** 267001 (2023).

[4] F. Bao et al., Phys. Rev. Lett. **129,** 010502 (2022).

[5] E. Dogan, D. Rosenstock, L. Le Guevel, H. Xiong, R. A. Mencia, A. Somoroff, K. N. Nesterov, M. G. Vavilov, V. E. Manucharyan, and C. Wang, Phys. Rev. Appl. **20,** 024011 (2023).

[6] I. N. Moskalenko, I. A. Simakov, N. N. Abramov, A. A. Grigorev, D. O. Moskalev, A. A. Pishchimova, N. S. Smirnov, E. V. Zikiy, I. A. Rodionov, and I. S. Besedin, npj Quantum Inf. **8,** 130 (2022).

[7] L. Ding, M. Hays, Y. Sung, B. Kannan, J. An, A. Di Paolo, A. H. Karamlou, T. M. Hazard, K. Azar, D. K. Kim, B. M. Niedzielski, A. Melville, M. E. Schwartz, J. L. Yoder, T. P. Orlando, S. Gustavsson, J. A. Grover, K. Serniak, and W. D. Oliver, Phys. Rev. X **13,** 031035 (2023).

[8] H. Zhang, C. Ding, D. K. Weiss, Z. Huang, Y. Ma, C. Guinn, S. Sussman, S. P. Chitta, D. Chen, A. A. Houck, J. Koch, and D. I. Schuster, arXiv:2309.05720.

[9] Y.-H. Lin, L. B. Nguyen, N. Grabon, J. San Miguel, N. Pankratova, and V. E. Manucharyan, Phys. Rev. Lett. **120,** 150503 (2018).

[10] H. Sun, F. Wu, H.-S. Ku, X. Ma, J. Qin, Z. Song, T. Wang, G. Zhang, J. Zhou, Y. Shi, H.-H. Zhao, and C. Deng, Phys. Rev. Appl. **20,** 034016 (2023).

[11] J. Koch, T. M. Yu, J. Gambetta, A. A. Houck, D. I. Schuster, J. Majer, A. Blais, M. H. Devoret, S. M. Girvin, and R. J. Schoelkopf, Phys. Rev. A **76,** 042319 (2007).

[12] Q. Ficheux, L. B. Nguyen, A. Somoroff, H. Xiong, K. N. Nesterov, M. G. Vavilov, and V. E. Manucharyan, Phys. Rev. X **11,** 021026 (2021).

[13] H. Xiong, Q. Ficheux, A. Somoroff, L. B. Nguyen, E. Dogan, D. Rosenstock, C. Wang, K. N. Nesterov, M. G. Vavilov, and V. E. Manucharyan, Phys. Rev. Res. **4,** 023040 (2022).

[14] I. A. Simakov, G. S. Mazhorin, I. N. Moskalenko, N. N. Abramov, A. A. Grigorev, D. O. Moskalev, A. A. Pishchimova, N. S. Smirnov, E. V. Zikiy, I. A. Rodionov, and I. S. Besedin, PRX Quantum **4,** 040321 (2023).

[15] L. B. Nguyen, G. Koolstra, Y. Kim, A. Morvan, T. Chistolini, S. Singh, K. N. Nesterov, C. Jünger, L. Chen, Z. Pedramrazi, B. K. Mitchell, J. M. Kreikebaum, S. Puri, D. I. Santiago, and I. Siddiqi, PRX Quantum **3,** 037001 (2022).

[16] A. J. Leggett, S. Chakravarty, A. T. Dorsey, M. P. Fisher, A. Garg, and W. Zwerger, Rev. Mod. Phys. **59,** 1 (1987).

[17] T. P. Orlando, J. E. Mooij, L. Tian, C. H. van der Wal, L. S. Levitov, S. Lloyd, and J. J. Mazo, Phys. Rev. B **60,** 15398 (1999).

[18] See Supplemental Material at http://link.aps.org/supplemental/10.1103/PhysRevLett.132.060602 for the detail analysis of the system's Hamiltonian, the impacts of the dynamics coupling, and the gate calibration and dominant errors, which includes Refs. [19–36].

[19] S. Gustavsson, F. Yan, G. Catelani, J. Bylander, A. Kamal, J. Birenbaum, D. Hover, D. Rosenberg, G. Samach, A. P. Sears, S. J. Weber, J. L. Yoder, J. Clarke, A. J. Kerman, F. Yoshihara, Y. Nakamura, T. P. Orlando, and W. D. Oliver, Science **354,** 1573 (2016).

[20] R. Barends, J. Kelly, A. Megrant, D. Sank, E. Jeffrey, Y. Chen, Y. Yin, B. Chiaro, J. Mutus, C. Neill, P. O'Malley, P. Roushan, J. Wenner, T. C. White, A. N. Cleland, and J. M. Martinis, Phys. Rev. Lett. **111,** 080502 (2013).

[21] P. V. Klimov et al., Phys. Rev. Lett. **121,** 090502 (2018).

[22] D. Ding, H.-S. Ku, Y. Shi, and H.-H. Zhao, Phys. Rev. B **103,** 174501 (2021).

[23] G. Zhang, Y. Liu, J. J. Raftery, and A. A. Houck, npj Quantum Inf. **3,** 1 (2017).

[24] M. H. S. Amin, Phys. Rev. Lett. **102,** 220401 (2009).

[25] G. Ithier, E. Collin, P. Joyez, P. J. Meeson, D. Vion, D. Esteve, F. Chiarello, A. Shnirman, Y. Makhlin, J. Schriefl, and G. Schön, Phys. Rev. B **72,** 134519 (2005).

[26] J. Bylander, S. Gustavsson, F. Yan, F. Yoshihara, K. Harrabi, G. Fitch, D. G. Cory, Y. Nakamura, J.-s. Tsai, and W. D. Oliver, Nat. Phys. **7,** 565 (2011).

[27] Z. Huang, P. S. Mundada, A. Gyenis, D. I. Schuster, A. A. Houck, and J. Koch, Phys. Rev. Appl. **15,** 034065 (2021).

[28] L. Landau, Phys. Z. Sowjetunion **2,** 46 (1932).

[29] C. Zener, Proc. R. Soc. A **137,** 696 (1932).

[30] J. M. Martinis and M. R. Geller, Phys. Rev. A **90,** 022307 (2014).

[31] J. Ghosh, A. Galiautdinov, Z. Zhou, A. N. Korotkov, J. M. Martinis, and M. R. Geller, Phys. Rev. A **87,** 022309 (2013).

[32] D. C. McKay, C. J. Wood, S. Sheldon, J. M. Chow, and J. M. Gambetta, Phys. Rev. A **96,** 022330 (2017).

[33] J. Kelly *et al.*, Phys. Rev. Lett. **112,** 240504 (2014).

[34] C. Neill *et al.*, Science **360,** 195 (2018).

[35] F. Arute *et al.*, Nature (London) **574,** 505 (2019).

[36] P. J. J. O'Malley *et al.*, Phys. Rev. Appl. **3,** 044009 (2015).

[37] X. Wu, J. L. Long, H. S. Ku, R. E. Lake, M. Bal, and D. P. Pappas, Appl. Phys. Lett. **111,** 2 (2017).

[38] J. E. Mooij, T. P. Orlando, L. Levitov, L. Tian, C. H. van der Wal, and S. Lloyd, Science **285,** 1036 (1999).

[39] B. L. T. Plourde, J. Zhang, K. B. Whaley, F. K. Wilhelm, T. L. Robertson, T. Hime, S. Linzen, P. A. Reichardt, C.-E. Wu, and J. Clarke, Phys. Rev. B **70,** 140501(R) (2004).

[40] C. Rigetti, A. Blais, and M. Devoret, Phys. Rev. Lett. **94,** 240502 (2005).

[41] P. Bertet, C. J. P. M. Harmans, and J. E. Mooij, Phys. Rev. B **73,** 064512 (2006).

[42] A. O. Niskanen, Y. Nakamura, and J. S. Tsai, Phys. Rev. B **73,** 094506 (2006).

[43] A. J. Kerman and W. D. Oliver, Phys. Rev. Lett. **101,** 070501 (2008).

[44] S. H. W. van der Ploeg, A. Izmalkov, A. M. van den Brink, U. Hübner, M. Grajcar, E. Il'ichev, H.-G. Meyer, and A. M. Zagoskin, Phys. Rev. Lett. **98,** 057004 (2007).

[45] R. Harris, A. J. Berkley, M. W. Johnson, P. Bunyk, S. Govorkov, M. C. Thom, S. Uchaikin, A. B. Wilson, J. Chung, E. Holtham, J. D. Biamonte, A. Y. Smirnov, M. H. S. Amin, and A. Maassen Van Den Brink, Phys. Rev. Lett. **98,** 177001 (2007).

[46] M. W. Johnson *et al.*, Nature (London) **473,** 194 (2011).

[47] S. J. Weber, G. O. Samach, D. Hover, S. Gustavsson, D. K. Kim, A. Melville, D. Rosenberg, A. P. Sears, F. Yan, J. L. Yoder, W. D. Oliver, and A. J. Kerman, Phys. Rev. Appl. **8,** 014004 (2017).

[48] A. O. Niskanen, K. Harrabi, F. Yoshihara, Y. Nakamura, S. Lloyd, and J. S. Tsai, Science **316,** 723 (2007).

[49] P. C. de Groot, J. Lisenfeld, R. N. Schouten, S. Ashhab, A. Lupaşcu, C. J. P. M. Harmans, and J. E. Mooij, Nat. Phys. **6,** 763 (2010).

[50] E. Paladino, Y. M. Galperin, G. Falci, and B. L. Altshuler, Rev. Mod. Phys. **86,** 361 (2014).

[51] L. B. Nguyen, Y.-H. Lin, A. Somoroff, R. Mencia, N. Grabon, and V. E. Manucharyan, Phys. Rev. X **9,** 041041 (2019).

[52] N. Didier, J. Bourassa, and A. Blais, Phys. Rev. Lett. **115,** 203601 (2015).

[53] C. Rigetti and M. Devoret, Phys. Rev. B **81,** 134507 (2010).

[54] L. Viola and S. Lloyd, Phys. Rev. A **58,** 2733 (1998).

[55] M. J. Biercuk, H. Uys, A. P. VanDevender, N. Shiga, W. M. Itano, and J. J. Bollinger, Nature (London) **458,** 996 (2009).

[56] M. A. Rol, F. Battistel, F. K. Malinowski, C. C. Bultink, B. M. Tarasinski, R. Vollmer, N. Haider, N. Muthusubramanian, A. Bruno, B. M. Terhal, and L. DiCarlo, Phys. Rev. Lett. **123,** 120502 (2019).

[57] V. Negîrneac, H. Ali, N. Muthusubramanian, F. Battistel, R. Sagastizabal, M. S. Moreira, J. F. Marques, W. J. Vlothuizen, M. Beekman, C. Zachariadis, N. Haider, A. Bruno, and L. DiCarlo, Phys. Rev. Lett. **126,** 220502 (2021).

[58] E. Magesan, J. M. Gambetta, B. R. Johnson, C. A. Ryan, J. M. Chow, S. T. Merkel, M. P. da Silva, G. A. Keefe, M. B. Rothwell, T. A. Ohki, M. B. Ketchen, and M. Steffen, Phys. Rev. Lett. **109,** 080505 (2012).

[59] R. Barends *et al.*, Nature (London) **508,** 500 (2014).

[60] D. K. Weiss, H. Zhang, C. Ding, Y. Ma, D. I. Schuster, and J. Koch, PRX Quantum **3,** 040336 (2022).